The 6th International Workshop on Advanced Smart Materials and Smart Structures Technology
ANCRiSST2011
July 25-26, 2011, Dalian, China

Decentralized $\mathcal{H}_2$ Controller Design for Civil Structures through Double Homotopy Transformation

Chunxu Qu [1, 2] , Yang Wang [2], Kincho H. Law [3], Hongnan Li [1]

[1] *School of Civil Engineering, Dalian University of Technology, Dalian 116024, China*
[2] *School of Civil and Environmental Engineering, Georgia Institute of Technology, Atlanta, GA 30332, USA*
[3] *Department of Civil and Environmental Engineering, Stanford University, Stanford, CA 94305, USA*

ABSTRACT

Traditional structural control systems usually employ a centralized controller that requires measurement data from all sensors in the entire structure, and makes control decisions for all control devices. The installation of a centralized control system in a large scale structure can be prohibitively expensive, and the long latency in a centralized system can cause poor control performance. As an alternative to centralized control, decentralized control architectures can be adopted, allowing control decisions based upon sensor data only from the vicinity of a control device, possibly transmitted via wireless communication. This paper presents a time-delayed decentralized $\mathcal{H}_2$ controller design for large-scale feedback structural control. The decentralized $\mathcal{H}_2$ controller design is achieved through double homotopy transformation method. The bilinear matrix inequality (BMI) describing the $\mathcal{H}_2$ control criteria is approximately linearized as a convex linear matrix inequality (LMI) problem, which can be solved by standard LMI solvers. The proposed algorithm is validated through numerical simulations with a six-story example structure.

INTRODUCTION

Civil structural control has been widely studied in recent decades [1-5]. A feedback control system contains sensors, controllers, and control devices (which can be active or semi-active). During external excitation, sensors collect structural vibration data, which is then transmitted to controllers. Controllers perform control decision making according to the sensor data, and command control devices to generate desired forces to suppress excessive structural responses. Traditional structural control systems usually employ a centralized controller that requires data from all sensors in the entire structure and makes control decisions for all control devices. The installation of a centralized control system in a large scale structure can be prohibitively expensive, and the long latency in a centralized system can cause poor control performance. As

an alternative to centralized control, decentralized control architectures can be adopted. A decentralized architecture allows control decisions to be made using sensor data only from the vicinity of a control device [6, 7]. By limiting data communication among nearby sensors and controllers, wireless devices can be a cost-effective alternative for the implementation of a feedback control system [8].

Towards decentralized structural control, Wang *et al*. [8] described a decentralized static output feedback control strategy that is based upon the linear quadratic regulator (LQR) criteria. Sparsity shape constraints are imposed on the gain matrices to represent decentralized feedback patterns, which reflect the communications among the nearby sensors. Iterative gradient method is adopted to search for decentralized gain matrices that optimize the control performance over the entire structure. Lu *et al*. [9] studied the performance of fully decentralized sliding mode control algorithms based on the stroke velocity and displacement measured on each control device itself to make control decision. Swartz and Lynch [10] presented a partially decentralized linear quadratic regulation control scheme that employs redundant state estimation as a means of minimizing the need for the communication of data between sensors. More recently, decentralized $\mathcal{H}_\infty$ controller design, taking into consideration of time delay due to communication and computing requirements, has also been explored [11, 12]. The decentralized controller design employs a homotopy method that gradually transforms a centralized controller into multiple decentralized controllers. Linear matrix inequality (LMI) constraints are included in the homotopic transformation to ensure optimal control performance. While LMI has many computational advantages, the general output feedback decentralized control problem is inherently a bilinear matrix inequality (BMI) problem. To deal with the BMI constraints, Mehendale and Grigoriadis proposed a double homotopy approach for decentralized $\mathcal{H}_\infty$ control in continuous-time domain [13].

This paper presents a time-delayed decentralized double homotopy approach that aims to minimize the $\mathcal{H}_2$ norm of the closed-loop system. The double homotopy algorithm is adapted from the continuous-time decentralized $\mathcal{H}_\infty$ control proposed in [13]. The algorithm is modified to consider inherent discrete communication and computing time delays for the decentralized $\mathcal{H}_2$ control formulation. Using this approach, a non-convex bilinear matrix inequality (BMI) describing the $\mathcal{H}_2$ control criteria is approximately linearized as a convex LMI problem, which can be computed by standard LMI solvers. The paper first introduces the problem formulation of decentralized structural control. The decentralized $\mathcal{H}_2$ control design through double homotopy transformation is then described. A six-story numerical example is provided to illustrate the performance of the time-delayed decentralized $\mathcal{H}_2$ controller design.

PROBLEM FORMULATION

Consider a structural control system with time delay shown in Figure 1. Following the derivations described in [11], the discrete-time open loop system can be formulated by concatenating the structural system and the system describing time delay and sensor noise as:

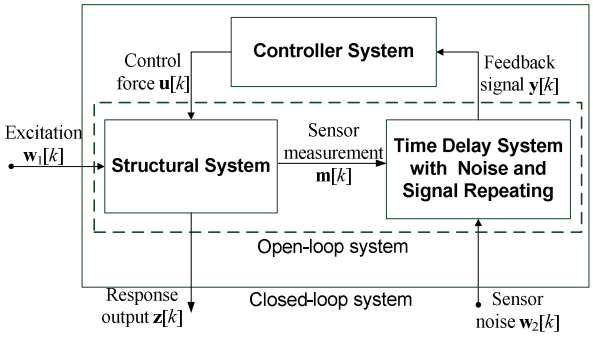

Figure 1. Diagram of the structural control system.

$$\begin{cases} \mathbf{x}[k+1] = \mathbf{A}\mathbf{x}[k] + \mathbf{B}_1\mathbf{w}[k] + \mathbf{B}_2\mathbf{u}[k] \\ \mathbf{z}[k] = \mathbf{C}_1\mathbf{x}[k] + \mathbf{D}_{11}\mathbf{w}[k] + \mathbf{D}_{12}\mathbf{u}[k] \\ \mathbf{y}[k] = \mathbf{C}_2\mathbf{x}[k] + \mathbf{D}_{21}\mathbf{w}[k] \end{cases} \quad (1)$$

where the system input $\mathbf{w} = [\mathbf{w}_1\ \mathbf{w}_2]^{\mathrm{T}} \in \mathbb{R}^{n_w \times 1}$ contains both external excitation $\mathbf{w}_1$ and sensor noise $\mathbf{w}_2$. Vector $\mathbf{u} \in \mathbb{R}^{n_u \times 1}$ denotes the control force vector. The open-loop state vector, $\mathbf{x} \in \mathbb{R}^{n_{OL} \times 1}$, contains $\mathbf{x}_S \in \mathbb{R}^{2n \times 1}$, the state vector of the structural system, and $\mathbf{x}_{TD} \in \mathbb{R}^{n_{TD} \times 1}$, the state vector of the time-delay and sensor noise system. For a lumped mass structural model with n stories, the state vector of the structural system, $\mathbf{x}_S$, consists of the relative displacement q_i and relative velocity $\dot{q}_i$ (with respect to the ground) for each floor i, $i = 1, \ldots n$.

$$\mathbf{x}_S = [q_1 \quad \dot{q}_1 \quad q_2 \quad \dot{q}_2 \quad \ldots \quad q_n \quad \dot{q}_n]^{\mathrm{T}} \quad (2)$$

The open-loop matrices $\mathbf{A} \in \mathbb{R}^{n_{OL} \times n_{OL}}$, $\mathbf{B}_1 \in \mathbb{R}^{n_{OL} \times n_w}$, and $\mathbf{B}_2 \in \mathbb{R}^{n_{OL} \times n_u}$ in Eq. (1) are, respectively, the state transition, the excitation influence, and the control influence matrices. Vector $\mathbf{z} \in \mathbb{R}^{n_z \times 1}$ represents the response output (to be controlled through the feedback loop), and $\mathbf{y} \in \mathbb{R}^{n_y \times 1}$ represents the time-delayed and noisy sensor signals. Correspondingly, the matrices $\mathbf{C}_1$, $\mathbf{D}_{11}$, and $\mathbf{D}_{12}$ are termed the output matrices, and the matrices $\mathbf{C}_2$ and $\mathbf{D}_{21}$ are the measurement matrices. Time delay of one sampling period ΔT is assumed for the sensor measurement signal (e.g. due to computational and/or communication latency). The formulation can be easily extended to model multiple time delay steps, as well as different time delays for different sensors.

To complete the feedback control loop, the controller system takes the time-delayed noisy signal $\mathbf{y}[k]$ as input and generates the desired (optimal) control force vector $\mathbf{u}[k]$, according to the following state-space equations:

$$\begin{cases} \mathbf{x}_G[k+1] = \mathbf{A}_G\mathbf{x}_G[k] + \mathbf{B}_G\mathbf{y}[k] \\ \mathbf{u}[k] = \mathbf{C}_G\mathbf{x}_G[k] + \mathbf{D}_G\mathbf{y}[k] \end{cases} \quad (3)$$

where $\mathbf{x}_G$ is the state vector of the controller system; $\mathbf{A}_G$, $\mathbf{B}_G$, $\mathbf{C}_G$, $\mathbf{D}_G$ are the parameter matrices of the controller which need to be determined during the optimal controller design.

DECENTRALIZED DISCRETE-TIME CONTROLLER DESIGN THROUGH DOUBLE HOMOTOPY TRANSFORMATION

This section first introduces the basic setup for decentralized control formulation, and then describes in detail how the controller decentralization is achieved through double homotopy transformation.

Decentralized Controller Setup

Decentralized controller dynamics can be described as a combination of decoupled controllers that operate separately and in parallel during the control process. Each controller only requires part of the measurement data. Mathematically, this is described by constraining the controller parameter matrices in Eq. (3) as block-diagonal matrices. This block-diagonal pattern allows Eq. (3) to be equivalent to the controller dynamics described in following decoupled equations:

$$
\begin{cases} \mathbf{x}_{G_I}[k+1] = \mathbf{A}_{G_I}\mathbf{x}_{G_I}[k] + \mathbf{B}_{G_I}\mathbf{y}_I[k] \\ \mathbf{u}_I[k] = \mathbf{C}_{G_I}\mathbf{x}_{G_I}[k] + \mathbf{D}_{G_I}\mathbf{y}_I[k] \end{cases}
$$
$$
\cdots,
$$
$$
\begin{cases} \mathbf{x}_{G_i}[k+1] = \mathbf{A}_{G_i}\mathbf{x}_{G_i}[k] + \mathbf{B}_{G_i}\mathbf{y}_i[k] \\ \mathbf{u}_i[k] = \mathbf{C}_{G_i}\mathbf{x}_{G_i}[k] + \mathbf{D}_{G_i}\mathbf{y}_i[k] \end{cases} \tag{4}
$$
$$
\cdots,
$$
$$
\begin{cases} \mathbf{x}_{G_N}[k+1] = \mathbf{A}_{G_N}\mathbf{x}_{G_N}[k] + \mathbf{B}_{G_N}\mathbf{y}_N[k] \\ \mathbf{u}_N[k] = \mathbf{C}_{G_N}\mathbf{x}_{G_N}[k] + \mathbf{D}_{G_N}\mathbf{y}_N[k] \end{cases}
$$

where $i = I...N$ is the sequence number of each decentralized controller; $\mathbf{x}_{G_i}$ is the state vector of the i-th decentralized controller; $\mathbf{u}_i$ is the i-th decentralized control force vector; $\mathbf{y}_i$ is the sensor signal available for the i-th decentralized controller. The decentralized control force and sensor signal are divisions of the complete force vector $\mathbf{u}$ and sensor signal $\mathbf{y}$ in Figure 1:

$$
\mathbf{y} = \begin{bmatrix} \mathbf{y}_I & \cdots & \mathbf{y}_i & \cdots & \mathbf{y}_N \end{bmatrix}^{\mathrm{T}} \tag{5a}
$$
$$
\mathbf{u} = \begin{bmatrix} \mathbf{u}_I & \cdots & \mathbf{u}_i & \cdots & \mathbf{u}_N \end{bmatrix}^{\mathrm{T}} \tag{5b}
$$

For convenience in later derivation, matrices $\tilde{\mathbf{A}}$, $\tilde{\mathbf{B}}_1$, $\tilde{\mathbf{B}}_2$, $\tilde{\mathbf{C}}_1$, $\tilde{\mathbf{C}}_2$, $\tilde{\mathbf{D}}_{11}$, $\tilde{\mathbf{D}}_{12}$, $\tilde{\mathbf{D}}_{21}$ are defined based on the open-loop system matrices in Eq. (1):

$$
\left[\begin{array}{c|c|c} \tilde{\mathbf{A}} & \tilde{\mathbf{B}}_1 & \tilde{\mathbf{B}}_2 \\ \hline \tilde{\mathbf{C}}_1 & \tilde{\mathbf{D}}_{11} & \tilde{\mathbf{D}}_{12} \\ \hline \tilde{\mathbf{C}}_2 & \tilde{\mathbf{D}}_{21} & \end{array}\right] \triangleq \left[\begin{array}{cc|c|cc} \mathbf{A} & \mathbf{0} & \mathbf{B}_1 & \mathbf{0} & \mathbf{B}_2 \\ \mathbf{0} & \mathbf{0} & \mathbf{0} & \mathbf{I}_{n_G} & \mathbf{0} \\ \hline \mathbf{C}_1 & \mathbf{0} & \mathbf{D}_{11} & \mathbf{0} & \mathbf{D}_{12} \\ \hline \mathbf{0} & \mathbf{I}_{n_G} & \mathbf{0} & & \\ \mathbf{C}_2 & \mathbf{0} & \mathbf{D}_{21} & & \end{array}\right] \tag{6}
$$

where n_G is the order of the controller system, which is equal to the order of the open loop system. The closed-loop system matrices can be derived by connecting the open-loop system and the controller system:

$$
\begin{cases} \mathbf{x}_{CL}[k+1] = \mathbf{A}_{CL}\mathbf{x}_{CL}[k] + \mathbf{B}_{CL}\mathbf{w}[k] \\ \mathbf{z}[k] = \mathbf{C}_{CL}\mathbf{x}_{CL}[k] + \mathbf{D}_{CL}\mathbf{w}[k] \end{cases} \tag{7a}
$$
$$
\mathbf{A}_{CL} = \tilde{\mathbf{A}} + \tilde{\mathbf{B}}_2\mathbf{G}\tilde{\mathbf{C}}_2 \tag{7b}
$$
$$
\mathbf{B}_{CL} = \tilde{\mathbf{B}}_1 + \tilde{\mathbf{B}}_2\mathbf{G}\tilde{\mathbf{D}}_{21} \tag{7c}
$$
$$
\mathbf{C}_{CL} = \tilde{\mathbf{C}}_1 + \tilde{\mathbf{D}}_{12}\mathbf{G}\tilde{\mathbf{C}}_2 \tag{7d}
$$
$$
\mathbf{D}_{CL} = \tilde{\mathbf{D}}_{11} + \tilde{\mathbf{D}}_{12}\mathbf{G}\tilde{\mathbf{D}}_{21} \tag{7e}
$$

where $\mathbf{G}$ is the combined controller matrix whose entries are the controller parameter matrices in Eq. (3):

$$\mathbf{G} = \begin{bmatrix} \mathbf{A}_G & \mathbf{B}_G \\ \mathbf{C}_G & \mathbf{D}_G \end{bmatrix} \tag{8}$$

Classical $\mathcal{H}_2$ controller designs provide centralized controllers that minimize the $\mathcal{H}_2$ norm of the closed-loop system. The $\mathcal{H}_2$ norm of the discrete-time closed-loop system is smaller than a given positive scalar γ, if and only if, there exist symmetric positive definite matrices **P** and **R** such that following matrix inequalities hold [14].

$$\begin{bmatrix} \mathbf{P} & \mathbf{P}\mathbf{A}_{CL} & \mathbf{P}\mathbf{B}_{CL} \\ * & \mathbf{P} & \mathbf{0} \\ * & * & \mathbf{I} \end{bmatrix} > 0 \tag{9a}$$

$$\begin{bmatrix} \mathbf{R} & \mathbf{C}_{CL} & \mathbf{D}_{CL} \\ * & \mathbf{P} & \mathbf{0} \\ * & * & \mathbf{I} \end{bmatrix} > 0 \tag{9b}$$

$$\text{Trace}(\mathbf{R}) < \gamma \tag{9c}$$

where * denotes a symmetric entry; ">0" means that the matrix at the left side of the inequality is positive definite.

Substituting the closed-loop system matrices from Eq. (7) into inequalities (9a) and (9b), the matrix variable $\mathbf{F}_1$ is defined as a function of **G** and **P**. $\mathbf{F}_2$ is defined as a function of **G**, **P**, and **R**.

$$\mathbf{F}_1(\mathbf{G},\mathbf{P}) = \begin{bmatrix} \mathbf{P} & \mathbf{P}\left(\tilde{\mathbf{A}} + \tilde{\mathbf{B}}_2\mathbf{G}\tilde{\mathbf{C}}_2\right) & \mathbf{P}\left(\tilde{\mathbf{B}}_1 + \tilde{\mathbf{B}}_2\mathbf{G}\tilde{\mathbf{D}}_{21}\right) \\ * & \mathbf{P} & \mathbf{0} \\ * & * & \mathbf{I} \end{bmatrix} > 0 \tag{10a}$$

$$\mathbf{F}_2(\mathbf{G},\mathbf{P},\mathbf{R}) = \begin{bmatrix} \mathbf{R} & \tilde{\mathbf{C}}_1 + \tilde{\mathbf{D}}_{12}\mathbf{G}\tilde{\mathbf{C}}_2 & \tilde{\mathbf{D}}_{11} + \tilde{\mathbf{D}}_{12}\mathbf{G}\tilde{\mathbf{D}}_{21} \\ * & \mathbf{P} & \mathbf{0} \\ * & * & \mathbf{I} \end{bmatrix} > 0 \tag{10b}$$

Therefore, the closed-loop $\mathcal{H}_2$ norm is smaller than γ, if and only if, there exist a controller matrix **G** and symmetric positive definite matrices **P** and **R** such that:

$$\mathbf{F}_1(\mathbf{G},\mathbf{P}) > 0, \mathbf{F}_2(\mathbf{G},\mathbf{P},\mathbf{R}) > 0, \text{ and Trace } (\mathbf{R}) < \gamma \tag{11}$$

Double Homotopy Transformation

The inequalities shown in Eq. (10a) led to a bilinear matrix inequality (BMI) problem because **P** and **G** are both unknown variables and they co-exist in a number of entries [15]. If the controller parameter matrices are not required to be block-diagonal, algorithms to compute a typical centralized controller exist [16]. However, with a block-diagonal pattern constraint to the controller matrices, there is no general off-the-shelf packages or numerical algorithms for the decentralized control design problem. The optimization problem becomes non-convex and NP hard; heuristic schemes are often necessary to solve the problem. Mehendale and Grigoriadis proposed a double homotopy method for solving the continuous-time decentralized $\mathcal{H}_\infty$ control

problem [13]. In this study, the double homotopy method is adapted and modified for the discrete-time decentralized $\mathcal{H}_2$ controller design with feedback time delay.

In the initial step (k = 0) of the double homotopy method, the centralized controller matrix $\mathbf{G}_C$ and its associated matrix $\mathbf{P}_C$ are first defined as:

$$\mathbf{G}_0 = \mathbf{G}_C = \mathbf{G}_{C,diag} + \mathbf{G}_{C,off} \tag{12a}$$

$$\mathbf{P}_0 = \mathbf{P}_C \tag{12b}$$

where $\mathbf{G}_{C,diag}$ represents the controller matrix with only the block-diagonals of the centralized controller matrices $\mathbf{A}_G$, $\mathbf{B}_G$, $\mathbf{C}_G$, and $\mathbf{D}_G$. The block-diagonal pattern satisfies the decentralized feedback requirement in Eq. (4). $\mathbf{G}_{C,off}$ represents the controller matrix with only the off-diagonal blocks. At each double homotopy step k (k = 1, 2, …, K), incremental changes are introduced to the double homotopy transformation process:

$$\lambda = 1/K \tag{13a}$$

$$\mathbf{G}_k = \mathbf{G}_{k-1} + \Delta\mathbf{G}_k - \lambda\mathbf{G}_{C,off} \tag{13b}$$

$$\mathbf{P}_k = \mathbf{P}_{k-1} + \Delta\mathbf{P}_k \tag{13c}$$

The decentralized constraint is applied to the increment $\Delta\mathbf{G}_k$ at every homotopy step. As a result, starting from $\mathbf{G}_0$ defined in Eq. (12a), when k approaches from 0 to K, the off-diagonal blocks are gradually removed from $\mathbf{G}_k$. At the end of the double homotopy transformation process, $\mathbf{G}_K$ approaches a decentralized controller with its $\mathbf{A}_G$, $\mathbf{B}_G$, $\mathbf{C}_G$, and $\mathbf{D}_G$ matrices being block-diagonal.

To ensure that the closed-loop $\mathcal{H}_2$ norm criterion is satisfied, at every k-th homotopy step, $\mathbf{G}$ and $\mathbf{P}$ in Eq. (11) are substituted with $\mathbf{G}_k$ and $\mathbf{P}_k$ in Eq. (13) such that the variables $\{\mathbf{G}_k, \mathbf{P}_k, \mathbf{R}_k, \gamma_k\}$ need to satisfy the inequalities in Eq. (11). Otherwise, the increment (λ) needs to be reduced. The basic idea of the double homotopy approach is to approximately linearize the BMI in Eq. (10a) into a linear matrix inequality (LMI). When substituting $\mathbf{G}_k$ and $\mathbf{P}_k$ into Eq. (10a), the product terms $\mathbf{P}_k\left(\tilde{\mathbf{A}} + \tilde{\mathbf{B}}_2\mathbf{G}_k\tilde{\mathbf{C}}_2\right)$ and $\mathbf{P}_k\left(\tilde{\mathbf{B}}_1 + \tilde{\mathbf{B}}_2\mathbf{G}_k\tilde{\mathbf{D}}_{21}\right)$, which are the cause of the bilinear inequality, are expanded and linearized. When $\Delta\mathbf{P}_k$ and $\Delta\mathbf{G}_k$ are small, it is reasonable to neglect the products that contain both terms. In other words, the product terms are approximated as:

$$\begin{aligned}
&\mathbf{P}_k\left(\tilde{\mathbf{A}} + \tilde{\mathbf{B}}_2\mathbf{G}_k\tilde{\mathbf{C}}_2\right) \\
&= \left(\mathbf{P}_{k-1} + \Delta\mathbf{P}_k\right)\left[\tilde{\mathbf{A}} + \tilde{\mathbf{B}}_2\left(\mathbf{G}_{k-1} + \Delta\mathbf{G}_k - \lambda\mathbf{G}_{C,off}\right)\tilde{\mathbf{C}}_2\right] \\
&= \mathbf{P}_{k-1}\left[\tilde{\mathbf{A}} + \tilde{\mathbf{B}}_2\left(\mathbf{G}_{k-1} - \lambda\mathbf{G}_{C,off}\right)\tilde{\mathbf{C}}_2\right] + \mathbf{P}_{k-1}\tilde{\mathbf{B}}_2\Delta\mathbf{G}_k\tilde{\mathbf{C}}_2 + \Delta\mathbf{P}_k\left[\tilde{\mathbf{A}} + \tilde{\mathbf{B}}_2\left(\mathbf{G}_{k-1} - \lambda\mathbf{G}_{C,off}\right)\tilde{\mathbf{C}}_2\right] + \Delta\mathbf{P}_k\tilde{\mathbf{B}}_2\Delta\mathbf{G}_k\tilde{\mathbf{C}}_2 \\
&\approx \mathbf{P}_{k-1}\bar{\mathbf{A}} + \mathbf{P}_{k-1}\tilde{\mathbf{B}}_2\Delta\mathbf{G}_k\tilde{\mathbf{C}}_2 + \Delta\mathbf{P}_k\bar{\mathbf{A}}
\end{aligned} \tag{14a}$$

$$\begin{aligned}
&\mathbf{P}_k\left(\tilde{\mathbf{B}}_1 + \tilde{\mathbf{B}}_2\mathbf{G}_k\tilde{\mathbf{D}}_{21}\right) \\
&= \left(\mathbf{P}_{k-1} + \Delta\mathbf{P}_k\right)\left[\tilde{\mathbf{B}}_1 + \tilde{\mathbf{B}}_2\left(\mathbf{G}_{k-1} + \Delta\mathbf{G}_k - \lambda\mathbf{G}_{C,off}\right)\tilde{\mathbf{D}}_{21}\right] \\
&= \mathbf{P}_{k-1}\left[\tilde{\mathbf{B}}_1 + \tilde{\mathbf{B}}_2\left(\mathbf{G}_{k-1} - \lambda\mathbf{G}_{C,off}\right)\tilde{\mathbf{D}}_{21}\right] + \mathbf{P}_{k-1}\tilde{\mathbf{B}}_2\Delta\mathbf{G}_k\tilde{\mathbf{D}}_{21} + \Delta\mathbf{P}_k\left[\tilde{\mathbf{B}}_1 + \tilde{\mathbf{B}}_2\left(\mathbf{G}_{k-1} - \lambda\mathbf{G}_{C,off}\right)\tilde{\mathbf{D}}_{21}\right] + \Delta\mathbf{P}_k\tilde{\mathbf{B}}_2\Delta\mathbf{G}_k\tilde{\mathbf{D}}_{21} \\
&\approx \mathbf{P}_{k-1}\bar{\mathbf{B}} + \mathbf{P}_{k-1}\tilde{\mathbf{B}}_2\Delta\mathbf{G}_k\tilde{\mathbf{D}}_{21} + \Delta\mathbf{P}_k\bar{\mathbf{B}}
\end{aligned} \tag{14b}$$

With the above approximation, the BMI problem is converted to an LMI problem where there is no cross multiplication involving $\Delta\mathbf{P}_k$ and $\Delta\mathbf{G}_k$. In addition, the two expressions in Eq. (10b) can be rewritten without the approximation as:

$$\begin{aligned}\tilde{\mathbf{C}}_1+\tilde{\mathbf{D}}_{12}\mathbf{G}_k\tilde{\mathbf{C}}_2 &= \tilde{\mathbf{C}}_1+\tilde{\mathbf{D}}_{12}\left(\mathbf{G}_{k\text{-}1}+\Delta\mathbf{G}_k-\lambda\mathbf{G}_{C,off}\right)\tilde{\mathbf{C}}_2 \\ &= \tilde{\mathbf{C}}_1+\tilde{\mathbf{D}}_{12}\left(\mathbf{G}_{k\text{-}1}-\lambda\mathbf{G}_{C,off}\right)\tilde{\mathbf{C}}_2+\tilde{\mathbf{D}}_{12}\Delta\mathbf{G}_k\tilde{\mathbf{C}}_2 \qquad (14c)\\ &= \bar{\mathbf{C}}+\tilde{\mathbf{D}}_{12}\Delta\mathbf{G}_k\tilde{\mathbf{C}}_2 \\ \tilde{\mathbf{D}}_{11}+\tilde{\mathbf{D}}_{12}\mathbf{G}_k\tilde{\mathbf{D}}_{21} &= \tilde{\mathbf{D}}_{11}+\tilde{\mathbf{D}}_{12}\left(\mathbf{G}_{k\text{-}1}+\Delta\mathbf{G}_k-\lambda\mathbf{G}_{C,off}\right)\tilde{\mathbf{D}}_{21} \\ &= \tilde{\mathbf{D}}_{11}+\tilde{\mathbf{D}}_{12}\left(\mathbf{G}_{k\text{-}1}-\lambda\mathbf{G}_{C,off}\right)\tilde{\mathbf{D}}_{21}+\tilde{\mathbf{D}}_{12}\Delta\mathbf{G}_k\tilde{\mathbf{D}}_{21} \qquad (14d)\\ &= \bar{\mathbf{D}}+\tilde{\mathbf{D}}_{12}\Delta\mathbf{G}_k\tilde{\mathbf{D}}_{21}\end{aligned}$$

Introducing the following new notations:

$$\bar{\mathbf{A}}=\tilde{\mathbf{A}}+\tilde{\mathbf{B}}_2\left(\mathbf{G}_{k\text{-}1}-\lambda\mathbf{G}_{C,off}\right)\tilde{\mathbf{C}}_2 \qquad (15a)$$

$$\bar{\mathbf{B}}=\tilde{\mathbf{B}}_1+\tilde{\mathbf{B}}_2\left(\mathbf{G}_{k\text{-}1}-\lambda\mathbf{G}_{C,off}\right)\tilde{\mathbf{D}}_{21} \qquad (15b)$$

$$\bar{\mathbf{C}}=\tilde{\mathbf{C}}_1+\tilde{\mathbf{D}}_{12}\left(\mathbf{G}_{k\text{-}1}-\lambda\mathbf{G}_{C,off}\right)\tilde{\mathbf{C}}_2 \qquad (15c)$$

$$\bar{\mathbf{D}}=\tilde{\mathbf{D}}_{11}+\tilde{\mathbf{D}}_{12}\left(\mathbf{G}_{k\text{-}1}-\lambda\mathbf{G}_{C,off}\right)\tilde{\mathbf{D}}_{21} \qquad (15d)$$

the three inequalities can be rewritten in terms of $\Delta\mathbf{G}_k$, $\Delta\mathbf{P}_k$, $\mathbf{R}_k$, and γ_k as follows:

$$\mathbf{V}_1(\Delta\mathbf{G}_k,\Delta\mathbf{P}_k) = \begin{bmatrix} \mathbf{P}_{k-1}+\Delta\mathbf{P}_k & \mathbf{P}_{k-1}\bar{\mathbf{A}}+\mathbf{P}_{k-1}\tilde{\mathbf{B}}_2\Delta\mathbf{G}_k\tilde{\mathbf{C}}_2+\Delta\mathbf{P}_k\bar{\mathbf{A}} & \mathbf{P}_{k-1}\bar{\mathbf{B}}+\mathbf{P}_{k-1}\tilde{\mathbf{B}}_2\Delta\mathbf{G}_k\tilde{\mathbf{D}}_{21}+\Delta\mathbf{P}_k\bar{\mathbf{B}} \\ * & \mathbf{P}_{k-1}+\Delta\mathbf{P}_k & \mathbf{0} \\ * & * & \mathbf{I}\end{bmatrix} > 0 \qquad (16a)$$

$$\mathbf{V}_2(\Delta\mathbf{G}_k,\Delta\mathbf{P}_k,\mathbf{R}_k) = \begin{bmatrix} \mathbf{R}_k & \bar{\mathbf{C}}+\tilde{\mathbf{D}}_{12}\Delta\mathbf{G}_k\tilde{\mathbf{C}}_2 & \bar{\mathbf{D}}+\tilde{\mathbf{D}}_{12}\Delta\mathbf{G}_k\tilde{\mathbf{D}}_{21} \\ * & \mathbf{P}_{k-1}+\Delta\mathbf{P}_k & \mathbf{0} \\ * & * & \mathbf{I}\end{bmatrix} > 0 \qquad (16b)$$

$$\text{Trace}(\mathbf{R}_k) < \gamma_k \qquad (16c)$$

The procedure searching for a decentralized controller $\mathbf{G}_D$ from a centralized controller $\mathbf{G}_C$ can now be summarized below.

Step 1: Compute variables $\mathbf{P}_C$ and γ_C associated with the centralized controller $\mathbf{G}_C$. Define $\mathbf{G}_{C,diag}$ and $\mathbf{G}_{C,off}$ as described in Eq. (12a). Set $\gamma_0 \leftarrow \gamma_C$, and set an upper limit (γ_{max}) for γ, e.g. $2^5\,\gamma_C$.

Step 2: Initialize the total number of double homotopy steps as K (e.g. 2^7); set an upper limit (K_{max}) for K, e.g. 2^{13}; set $\lambda = 1/K$, $k \leftarrow 1$, $\mathbf{P}_0 \leftarrow \mathbf{P}_C$, $\mathbf{G}_0 \leftarrow \mathbf{G}_C$.

Step 3: At step k, solve the following LMI problem with variables $\Delta\mathbf{P}_k$, $\Delta\mathbf{G}_k$ (block-diagonal pattern), $\mathbf{R}_k$, and γ_k.

$$\begin{aligned} &\text{minimize} \quad \gamma_k \\ &\text{subject to} \quad \mathbf{V}_1(\Delta\mathbf{G}_k, \Delta\mathbf{P}_k) > 0,\ \mathbf{V}_2(\Delta\mathbf{G}_k, \Delta\mathbf{P}_k, \mathbf{R}_k) > 0,\ \text{Trace}(\mathbf{R}_k) < \gamma_k, \\ &\qquad \|\Delta\mathbf{P}_k\| < \lambda\|\mathbf{P}_{k-1}\|,\ \|\Delta\mathbf{G}_k\| < \lambda\|\mathbf{G}_C\|,\ \gamma_k \geq \gamma_{k-1}. \end{aligned} \tag{17}$$

Step 4: Set $\mathbf{G}_k = \mathbf{G}_{k-1} + \Delta\mathbf{G}_k - \lambda\mathbf{G}_{C,off}$ and $\mathbf{P}_k = \mathbf{P}_{k\text{-}1} + \Delta\mathbf{P}_k$. Check that the solutions $\mathbf{G}_k, \mathbf{P}_k, \mathbf{R}_k, \gamma_k$ satisfy Eq. (11). If they do, set $k \leftarrow k$+1 and go to Step 5. If not, set $k \leftarrow 1$ and $K \leftarrow 2K$. If $K<K_{max}$, repeat Step 2; otherwise set $\gamma_0 \leftarrow s_\gamma\gamma_C$ (s_γ is a relaxation factor that is greater than one) under the constraint $\gamma_0 \leq \gamma_{max}$ and restart from Step 2. If $\gamma_0 > \gamma_{max}$, it is concluded that the algorithm does not converge.

Step 5: If k=K, the desired decentralized $\mathcal{H}_2$ controller is given by $\mathbf{G}_K$; otherwise set $k \leftarrow k$+1, and go to Step 2.

It should be noted that the algorithm described above is heuristic in nature and does not guarantee convergence. In addition, non-convergence does not imply the non-existence of a decentralized $\mathcal{H}_2$ controller.

NUMERICAL EXAMPLE

This section discusses the decentralized $\mathcal{H}_2$ structural control design problem using a six-story example structure. Numerical simulations are conducted to demonstrate the performance of different decentralized and centralized feedback architectures.

Formulation of the Six-story Example Structure

A six-story numerical example as shown in Figure 2(a) is used to validate the performance of the decentralized controllers. The in-plane lumped-mass model is based on a laboratory structure constructed by researchers at the National Center for Research on Earthquake Engineering (NCREE) in Taiwan [9]. The floor plan is 1.0 m by 1.5 m and the story height is 1.0 m. In this simulation study, one actuator is allocated on each of the 1st, 3rd, and 5th floor. Through a V-brace, every actuator applies horizontal force between two neighboring floors.

Considering that excessive inter-story drifts are of concern, the output matrices of the structural system are defined such that the 2-norm of the output vector $\mathbf{z}[k]$ is a quadratic function of the inter-story drifts and the control forces:

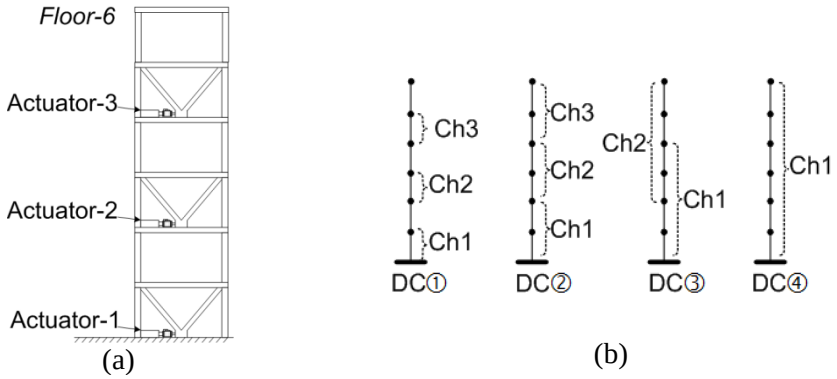

(a) (b)

Figure 2. A six-story model structure: (a) deployment of three actuators; (b) communication architecture for different degrees of centralization (DC).

$$\left\|\mathbf{z}[k]\right\|_2^2 = 10^4\left[\left(q_1[k]\right)^2 + \sum_{i=2}^{6}\left(q_i[k]-q_{i-1}[k]\right)^2\right] + 10^{-9}\sum_{i=1}^{3}u_i^2[k] \tag{18}$$

The $\mathcal{H}_2$ controller design aims to minimize the closed-loop $\mathcal{H}_2$-norm, $\left\|\mathbf{H}_{\mathbf{zw}}\right\|_2$, which is the system norm from the input **w** (including ground excitation $\mathbf{w}_1$ and sensor noises $\mathbf{w}_2$) to the output **z**. In addition, it is assumed that inter-story drifts can be measured. Accordingly, the measurement matrices of the structural system are defined such that the measurement vector **m**[*k*] is given as follows.

$$\mathbf{m}[k] = \begin{bmatrix} q_1[k] & q_2[k]-q_1[k] & \cdots & q_6[k]-q_5[k] \end{bmatrix}^{\mathrm{T}} \tag{19}$$

Decentralized Control with Different Feedback Architectures

As illustrated in Figure 2(b), different control feedback architectures are designed for different degrees of centralization (DC). A larger number of DC represents a higher level of centralization. In each feedback architecture, one or more communication subnets exist, with each communication subnet (as denoted by channels Ch1, Ch2, etc.) covering a limited number of stories. The controllers covered by a subnet are allowed to access the sensor data within that subnet. For example, case DC ① implies that each subnet covers only one story and a total of three subnets exist; case DC ② implies that each subnet covers two stories and a total of three subnets exist. For case DC ③, each subnet covers four stories and the two communication channels overlap at the 3rd and 4th stories, representing a decentralized architecture with information overlapping. For DC ④, one subnet covers all six stories, which results in a centralized information architecture.

In practice, the control sampling time step for each control architecture is determined by the time required for communication and embedded computing (for example, using low cost wireless sensor devices [8,11]). To simulate this effect, time delay is approximated as one sampling time step ΔT (in accordance with the formulation in Figure 1). Due to different requirements on communication and computing, the shortest sampling time step ΔT that can be achieved by each control architecture may be different. Because case DC ① requires minimum amount of computing, its 15ms time step (i.e. time delay) is the smallest. Cases DC ② and DC ③ require more communication and computing, and thus, have a time step of 20ms and 25ms, respectively. Due to the largest amount of communication and computing required by the centralized pattern, case DC ④ has the longest time step of 52ms. The time delays are summarized in Table 1.

Table 1 Feedback time delays for four different controllers

	DC ①	DC ②	DC ③	DC ④
Time delay (ms)	15	20	25	52

The 1940 El Centro NS (Imperial Valley Irrigation District Station) earthquake excitation with the peak ground acceleration (PGA) scaled to 1m/s^2 is employed in this study. Figure 3(a) shows the peak inter-story drifts for different control architectures as well as for the uncontrolled structure during the ground excitation. All controllers can successfully reduce structural response compared to the case without control. Figure 3(b) shows the RMS (root-mean-square) inter-story drifts for the four control cases. The case without control has an RMS drift of 2.5×10^{-3}m at the 2nd story, which is much larger than any of the control cases. For clarity, the case without control is excluded from the plot in Figure 3(b). Among the four control cases, the decentralized cases DC ② and DC ③ achieve less inter-story drifts that are more uniformly distributed over the

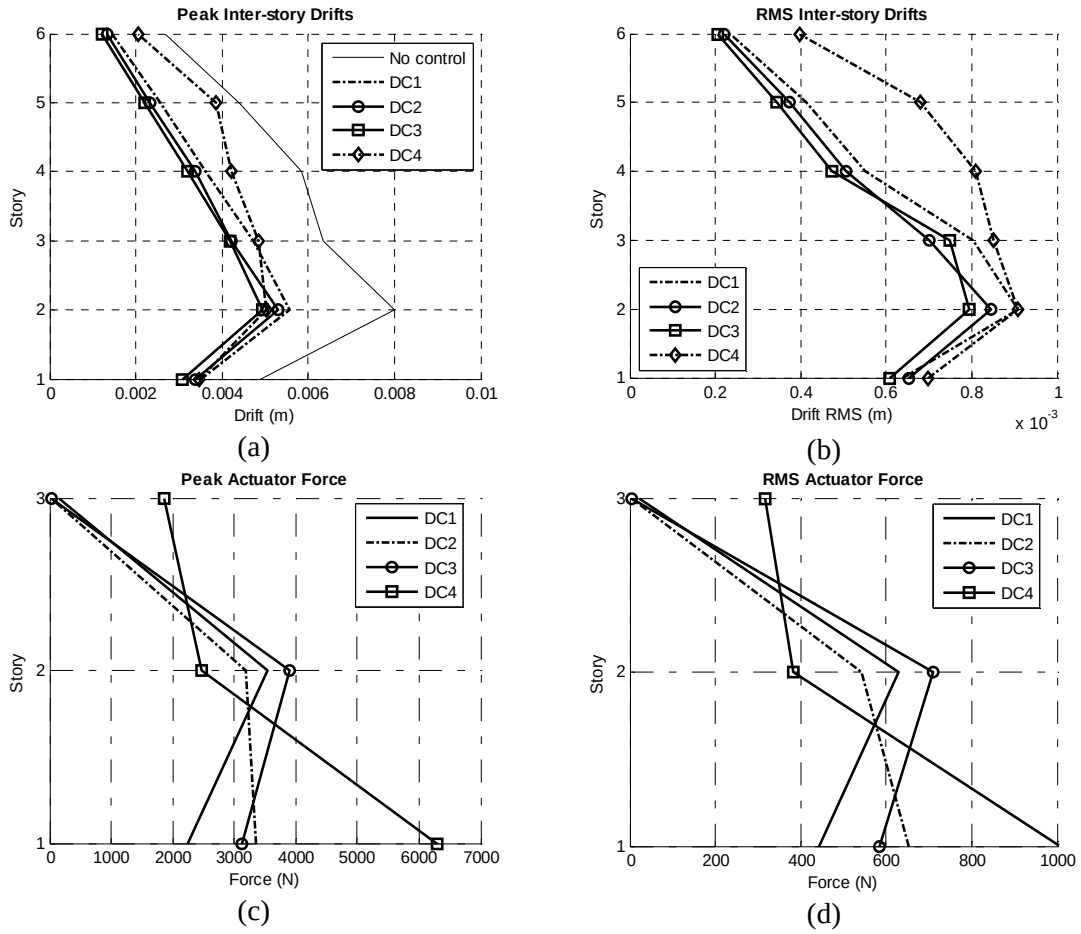

Figure 3. Simulation results for decentralized and centralized control: (a) peak inter-story drifts; (b) RMS inter-story drifts; (c) peak actuator forces; (d) RMS actuator forces.

structure. On the other hand, case DC④ shows the "worst" control performance with the largest RMS inter-story drifts. Such difference in control performance is mainly caused by the different time delays of different control architectures.

For practical applications of feedback structural control, one of the major constraints is the capacity of realistic semi-active or active control devices. Compared with the ideal actuators adopted in this study, a realistic control device may not be able to deliver a desired force with large magnitude. Figure 3(c) shows the peak actuator forces required by different control architectures, and Figure 3(d) shows the RMS forces. Both plots illustrate case DC④ has the highest requirement on actuator force, particularly at the base story.

SUMMARY AND CONCLUSION

This paper presents a decentralized controller design that minimizes the closed-loop $\mathcal{H}_2$ norm in structural control. The problem is studied in discrete-time domain with time delay. The decentralized controller is computed through a double homotopy method, which deforms a centralized controller to a decentralized pattern. The non-convex bilinear matrix inequality (BMI) problem is approximately solved by linearizing it to a linear matrix inequality (LMI) problem.

The performance of the decentralized controller design is validated using numerical simulation with a six-story structure. It is shown that when the time delay is acceptable, the more

measurement data is communicated to the decentralized controllers, the better the performance is. This is illustrated by comparing decentralized cases DC② and DC③ versus decentralized case DC①. On the other hand, more data communication and computation can cause larger time delay. The centralized controller DC④ used in the simulation has the most data available, but its control performance is inferior due to the significantly longer time delay.

ACKNOWLEDGEMENT

This work was partially supported by NSF, Grant Number CMMI-0824977, awarded to Prof. Kincho H. Law of Stanford University. The authors would like to thank Prof. Chin-Hsiung Loh and Dr. Kung-Chun Lu of the National Taiwan University, as well as Dr. Pei-Yang Lin of NCREE, for generously providing the numerical model of the six-story example structure. Any opinions, findings and conclusions expressed in this paper are those of the authors and do not necessarily reflect the views of their collaborators and the National Science Foundation.

REFERENCES

[1] T. T. Soong, *Active Structural Control: Theory and Practice*. Harlow, Essex, England: Wiley, 1990.

[2] B. F. Spencer, Jr. and S. Nagarajaiah, State of the art of structural control, *Journal of Structural Engineering,* 129(7), 845-856, 2003.

[3] J. T. P. Yao, Concept of structural control, *Journal of Structural Division, ASCE,* 98(7), 1567-1574, 1972.

[4] G. W. Housner, L. A. Bergman, T. K. Caughey, A. G. Chassiakos, R. O. Claus, S. F. Masri, R. E. Skelton, T. T. Soong, B. F. Spencer, Jr., and J. T. P. Yao, Structural control: past, present, and future, *Journal of Engineering Mechanics,* 123(9), 897-971, 1997.

[5] S. Y. Chu, T. T. Soong, and A. M. Reinhorn, *Active, Hybrid, and Semi-active Structural Control: a Design and Implementation Handbook*. Hoboken, NJ: Wiley, 2005.

[6] N. Sandell, Jr., P. Varaiya, M. Athans, and M. Safonov, Survey of decentralized control methods for large scale systems, *Automatic Control, IEEE Transactions on,* 23(2), 108-128, 1978.

[7] D. D. Siljak, *Decentralized Control of Complex Systems*. Boston: Academic Press, 1991.

[8] Y. Wang, R. A. Swartz, J. P. Lynch, K. H. Law, K.-C. Lu, and C.-H. Loh, Decentralized civil structural control using real-time wireless sensing and embedded computing, *Smart Structures and Systems,* 3(3), 321-340, 2007.

[9] K.-C. Lu, C.-H. Loh, J. N. Yang, and P.-Y. Lin, Decentralized sliding mode control of a building using MR dampers, *Smart Materials and Structures,* 17(5), 055006, 2008.

[10] R. A. Swartz and J. P. Lynch, Strategic network utilization in a wireless structural control system for seismically excited structures, *Journal of Structural Engineering,* 135(5), 597-608, 2009.

[11] Y. Wang, Time-delayed dynamic output feedback H_∞ controller design for civil structures: a decentralized approach through homotopic transformation, *Structural Control and Health Monitoring,* 18(2), 121-139, 2011.

[12] Y. Wang, K. H. Law, and S. Lall, Time-delayed decentralized H_∞ controller design for civil structures: a homotopy method through linear matrix inequalities, in *Proceedings of the 2009 American Control Conference (ACC 2009)*, St. Louis, MO, USA, 2009.

[13] C. S. Mehendale and K. M. Grigoriadis, A double homotopy method for decentralised control design, *International Journal of Control,* 81(10), 1600 - 1608, 2008.

[14] I. Masubuchi, A. Ohara, and N. Suda, LMI-based controller synthesis: A unified formulation and solution, *International Journal of Robust and Nonlinear Control,* 8(8), 669-686, 1998.

[15] J. G. VanAntwerp and R. D. Braatz, A tutorial on linear and bilinear matrix inequalities, *Journal of Process Control*, 10(4), 363-385, 2000.

[16] F. Paganini and E. Feron, *Linear matrix inequality methods for robust H_2 analysis: a survey with comparisons*, in *Advances in Linear Matrix Inequality Methods in Control: Advances in Design and Control*, L. E. Ghaoui and S.-l. Niculescu, Eds.: Society for Industrial and Applied Mathematics, 2000, 129-151.